

The Effect of Water on the Microstructure of 1-Butyl-3-methylimidazolium Tetrafluoroborate/TX-100/Benzene Ionic Liquid Microemulsions

Yan'an Gao, Na Li, Liqiang Zheng,* Xueyan Zhao, Jin Zhang, Quan Cao, Mingwei Zhao, Zhen Li, and Gaoyong Zhang^[a]

Abstract: The ionic liquid (IL) 1-butyl-3-methylimidazolium tetrafluoroborate ([bmim][BF₄]) forms nonaqueous microemulsions with benzene with the aid of nonionic surfactant TX-100. The phase diagram of the ternary system was prepared, and the microstructures of the microemulsion were recognized. On the basis of the phase diagram, a series of ionic liquid-in-oil (IL/O) microemulsions were chosen and characterized by dynamic light scattering (DLS), which shows a similar swelling behavior to typical water-in-oil (W/O) microemulsions. The existence of IL pools in the IL/O microemulsion was confirmed by UV/Vis spectroscopic

analysis with CoCl₂ and methylene blue (MB) as the absorption probes. A constant polarity of the IL pool is observed, even if small amounts of water are added to the microemulsion, thus suggesting that the water molecules are solubilized in the polar outer shell of the microemulsion, as confirmed by FTIR spectra. ¹H NMR spectroscopic analysis shows that these water molecules interact with the electronegative

oxygen atoms of the oxyethylene (OE) units of TX-100 through hydrogen-bonding interactions, and the electronegative oxygen atoms of the water molecules attract the electropositive imidazolium rings of [bmim][BF₄]. Hence, the water molecules are like a glue that stick the IL and OE units more tightly together and thus make the microemulsion system more stable. Considering the unique solubilization behavior of added water molecules, the IL/O microemulsion system may be used as a medium to prepare porous or hollow nanomaterials by hydrolysis reactions.

Keywords: dynamic light scattering • ionic liquids • IR spectroscopy • microemulsions • NMR spectroscopy • UV/Vis spectroscopy

Introduction

In recent years, microemulsions have been evaluated as a unique and versatile reaction medium for a variety of chemical reactions, such as nanoparticle preparation and organic or bioorganic synthesis.^[1–3] The majority of microemulsion studies use water as the polar component. However, substantial efforts have focused on the investigation of nonaqueous microemulsions.^[4–8] In these investigations, water was replaced by polar nonaqueous solvents, such as ethylene glycol, formamide, glycerol, and *N,N*-dimethylformamide, which are immiscible with hydrocarbon solvents.^[9] These nonaqueous microemulsions have attracted much interest

from both theoretical and practical viewpoints^[6] and have been widely applied to cosmetics, solar energy conversion, semiconductors, and microcolloids.^[10] Furthermore, there seems to be a number of distinct advantages to nonaqueous microemulsion systems over the aqueous systems; for example, nonaqueous systems often show much larger stability regions in isotropic solutions relative to the analogous aqueous systems.^[11] A large variety of different surfactants can be used to give nonaqueous microemulsions.^[12] Moreover, these microemulsions are useful media for organic reactions, such as the Diels–Alder reaction, esterification, and polymerization.^[13–20] These microemulsions are, of course, particularly attractive for those reactants that must avoid contact with water.

Ionic liquids (ILs) have recently attracted interest as environmentally benign solvents for synthesis^[21–23] or extraction.^[24] Owing to their ionic character, ILs usually display extremely low vapor pressures. Accordingly, the increased use of ILs instead of traditional organic solvents results in significantly less evaporation of volatile organic compounds. Therefore, ILs have widely been classified as “green sol-

[a] Dr. Y. Gao, N. Li, Prof. L. Zheng, X. Zhao, Dr. J. Zhang, Q. Cao, M. Zhao, Z. Li, Prof. G. Zhang
Key Laboratory of Colloid and Interface Chemistry
Shandong University, Ministry of Education
Jinan 250100 (China)
Fax: (+86)531-88564750
E-mail: lqzheng@sdu.edu.cn

vents”, although certain aspects of their environmental safety have yet to be clarified.^[21]

The use of ILs instead of water to prepare a nonaqueous IL microemulsion is an active research field, and recently Han and co-workers discovered that 1-butyl-3-methylimidazolium tetrafluoroborate ([bmim][BF₄]) acts as polar nano-sized droplets dispersed in a continuous hydrocarbon solvent.^[25] Freeze–fracture transmission electron microscopy (FFTEM) indicated a droplet structure which takes the same shape as “classic” water-in-oil (W/O) microemulsions.^[25] Eastoe et al. investigated the microemulsion system by small-angle neutron scattering (SANS), which showed a regular increase in droplet volume as the micelles were progressively swollen with added [bmim][BF₄], a behavior consistent with “classic” W/O microemulsions.^[26] In addition, the effects of confining [bmim][BF₄] to salvation dynamics and rotational relaxation of Coumarin 153 in TX-100/cyclohexane microemulsions have been explored by using steady-state and picosecond time-resolved emission spectroscopy.^[27] More recently, a study by us has indicated that the interaction between the electronegative oxygen atoms of the oxyethylene (OE) units of TX-100 and the electropositive imidazolium rings may be the driving force for the solubilization of [bmim][BF₄] into the core of the TX-100 aggregates.^[28]

These nonaqueous IL microemulsions are a new class of reaction media. They can overcome the solubility limitations of ILs in apolar solvents.^[26] Furthermore, nanostructured surfactant assemblies provide hydrophobic or hydrophilic nanodomains, thereby expanding the potential uses of ILs in microheterogeneous systems as reaction, separation, or extraction media.^[26] Also, microemulsions with ILs as the polar core dispersed in a continuous oil phase by a suitable surfactant may have some unknown properties and some potential applications owing to the unique features of ILs and microemulsions.^[25,27]

Despite their great potential, reports on the nonaqueous IL microemulsions, in particular on their microstructures, are still very scarce. Herein, we study the nonaqueous microemulsions of TX-100 in benzene with polar [bmim][BF₄] as a water substitute. The effect of a small amount of water on the microstructure of the IL/O microemulsion is investigated by the use of UV/Vis, FTIR, and ¹H NMR spectroscopic analysis, mainly because these techniques are noninvasive, functional-group selective, sensitive to chemical environments, and free of problems that arise from scattering experiments.^[29] The current studies can help to understand the microstructure of IL microemulsions and thus establish a better way of using them as a new medium.

Experimental Section

Materials: TX-100 was obtained from Alfa Aesar and evaporated under vacuum at 80 °C for 4 h to remove excess water before use. To avoid the atmospheric water, [bmim][BF₄] was freshly made and used. The containers with the materials were sealed tightly to avoid any further contact

with air before use. Methyl orange (MO), methylene blue (MB), cobalt chloride, and benzene were all provided by the Beijing Chemical Reagents Company (A.R. grade). D₂O (99.96 atom %) was purchased from the Shanghai Chemical Reagents Company. Water was doubly deionized and distilled. [bmim][BF₄] was synthesized according to standard methods by a quaternization reaction of 1-methylimidazole with 1-chlorobutane.^[30] The imidazolium chloride salt was crystallized in ethyl acetate at –30 °C. The postmetathesis product was obtained by ion exchange of 1-butyl-3-methylimidazolium chloride and potassium tetrafluoroborate in distilled water and then washed with dichloromethane and dried under a high vacuum. The purity of the product was checked by using ¹H NMR spectroscopic analysis.

Apparatus and procedures: The diameters of the [bmim][BF₄]/TX-100/benzene nonaqueous microemulsions were determined by dynamic light scattering (DLS; Brookhaven Instrument Co.: BI-200SM goniometer and BI-9000 AT correlator machines) with an argon-ion laser operating at 488 nm. The viscosity of the continuous phase for each mixture was first measured by a NDJ-1 rotating viscosimeter (Shanghai, China) with an accuracy of 1%. All measurements were made at the scattering angle of 90° at 25 °C. The critical micelle concentration of TX-100 in [bmim][BF₄] was measured using a Krüss K12 tension apparatus. FTIR spectra were recorded in KBr pellets with a resolution of 2 cm^{–1} using a BIORAD FTS-165 spectrometer. There was no evident sign that the KBr pellets were eroded by the addition of small amounts of water to the investigated system. ¹H NMR spectroscopic measurements were carried out with a Varian ARX 400 NMR spectrometer at 25 °C. The instrument was operated at a frequency of 400.13 MHz with tetramethylsilane as an internal reference. The UV/Vis spectra were measured at 25 °C with a TU-1901 UV spectrometer.

Results and Discussion

Phase behavior and dynamic light scattering (DLS): The phase behavior of the [bmim][BF₄]/TX-100/benzene ternary system at 25.0 °C is shown in Figure 1. A large single iso-

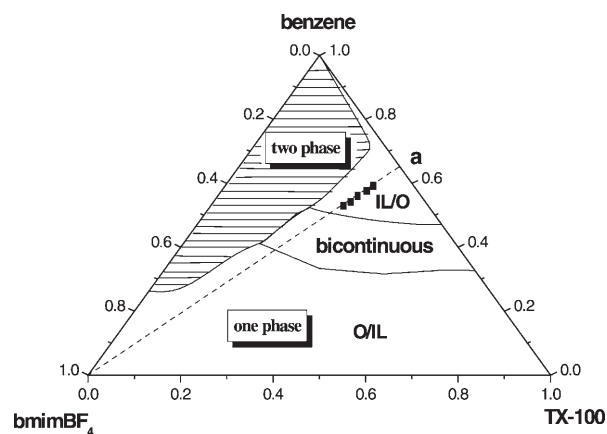


Figure 1. Phase diagram of the [bmim][BF₄]/TX-100/benzene three-component system at 25 °C. The initial TX-100 weight fraction is 0.35 for the line a.

tropic region that extends from the IL corner to the benzene corner is observed. The blank region marked “one phase” is the one-phase microemulsion, and the shadow region marked “two phase” is a turbid region, that is, a microemulsion in equilibrium with an excess the benzene or [bmim][BF₄] phase. It is evident that a continuous, stable single-

phase microemulsion region is always observed over the [bmim][BF₄] or benzene content range of 0–100 wt%. For traditional W/O microemulsions, on successively increasing the amount of water in suitable oil/surfactant binary systems, as long as there is no phase separation and the system remains isotropic, there should be some kind of gradual structural transition in the aqueous microemulsion.^[31] Similarly, in the current nonaqueous IL microemulsion system, the transition should span the range of possible structures from microdroplets to a bicontinuous structure. The microregions of [bmim][BF₄]-in-benzene (IL/O), bicontinuous, and benzene-in-[bmim][BF₄] (O/IL) were identified by electrical conductivity according to the recent reports.^[25,28]

Analysis with FFTEM shows a droplet structure for the [bmim][BF₄]-in-cyclohexane microemulsions.^[25] Small-angle neutron scattering (SANS) experiments further reveal ellipsoidal particles for the microemulsion because the ellipsoid model gives the best statistical fit, even relative to polydisperse spherical particles.^[26] Herein, DLS is used to evaluate the size and size distribution of the IL/O microemulsion droplets that are of interest because the nanometer-size IL microenvironments may find a wide range of applications.^[25] On the basis of the phase diagram, a series of samples in the IL/O microemulsion region along the dilute line a are chosen and characterized by DLS at various sample compositions (■). Figure 2 shows the size distribution of the

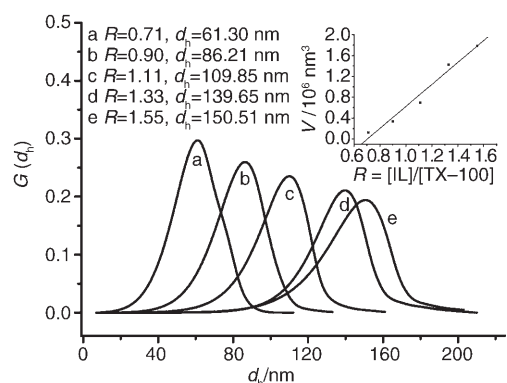


Figure 2. Size distributions of the [bmim][BF₄]-in-benzene microemulsion droplets given along line a in Figure 1 with a) $R=0.71$, b) 0.90, c) 1.11, d) 1.33, and e) 1.55. The sample compositions are marked with squares (■) in Figure 1. The inset shows the microemulsion-droplet-swelling behavior in terms of the dependence of ellipsoid volume V on R .

[bmim][BF₄]-in-benzene microemulsions. The size of the aggregates increased from 61.30 to 150.51 nm with increasing [IL]/[TX-100] molar ratio R from 0.71:1 to 1.55:1. The result is similar to those of typical W/O microemulsions, thus suggesting the formation of IL/O microemulsions.^[26] The inset in Figure 2 shows the microemulsion-droplet-swelling behavior in terms of the dependence of ellipsoid volume V on R . This regular swelling behavior is consistent with the volume of dispersed nanodomains being directly proportional to the amount of added IL, which is common to many droplet mi-

croemulsions such as W/O systems stabilized with sodium bis-2-ethylhexyl-sulfosuccinate (AOT).^[26,32]

The formation of IL pools: It is necessary to determine the formation of IL pools to study the influence of water on the microstructure of the IL/O microemulsion and delineate its actual locations in the microemulsion. For traditional aqueous microemulsions, the water molecules first hydrate the OE units of TX-100 when water is added to the TX-100-based reverse micellar solutions. After hydration has reached saturation, subsequently added water molecules accumulate in the core of the aggregates to form water pools, in which the water molecules have similar properties to bulk water.^[33] The water pools were intensively investigated by various technologies, such as FTIR and ¹H NMR spectroscopic analysis.^[2,33–36] In this section, we use two UV/Vis absorption probes, CoCl₂ and methylene blue (MB), to confirm the existence of IL pools.

The metal salt CoCl₂ was chosen mainly because it is insoluble in benzene but soluble in TX-100 and bulk [bmim][BF₄]. Thus, it can be concluded that CoCl₂ is completely solubilized in the polar cores of the [bmim][BF₄]-in-benzene (IL/O) microemulsions. More importantly, three remarkable characteristic peaks at 609, 633, and 660 nm appear (not shown herein) when CoCl₂ is added to pure [bmim][BF₄], whereas only one peak is observed at about 576 nm in the micellar aggregates of TX-100.^[37] Considering CoCl₂ is a highly ionic compound and requires a highly concentrated [bmim][BF₄] environment in which to dissolve, the common appearance of these three characteristic peaks is likely to indicate the formation of IL pools. Figure 3 shows the UV/Vis

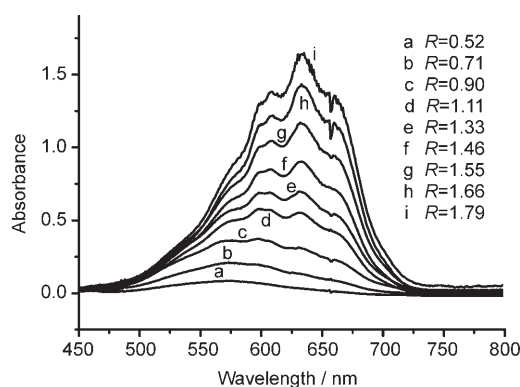


Figure 3. The UV/Vis absorption spectra of CoCl₂ in the [bmim][BF₄]-in-benzene nonaqueous IL microemulsions given along line a in Figure 1 with a) $R=0.52$, b) 0.71, c) 0.90, d) 1.11, e) 1.33, f) 1.46, g) 1.55, h) 1.66, and i) 1.79. CoCl₂ concentration: a) 0.4×10^{-3} , b) 0.8×10^{-3} , c) 1.2×10^{-3} , d) 1.6×10^{-3} , e) 2.0×10^{-3} , f) 2.4×10^{-3} , g) 2.8×10^{-3} , h) 3.2×10^{-3} , and i) 3.6×10^{-3} M.

absorption spectra of CoCl₂ solubilized in the IL/O reverse microemulsion as a function of added [bmim][BF₄] content. Evidently, at the [IL]/[TX-100] molar ratio $R < 1.11$, only one peak is observed, thus indicating that no bulk IL or bulk-like IL appears at this stage. Therefore, it can be de-

duced that [bmim][BF₄] molecules are bound to the OE units of TX-100. However, the three characteristic absorption peaks of CoCl₂ appear when $R > 1.11$, which is the same behavior as that of bulk [bmim][BF₄], thus revealing that CoCl₂ is solubilized in an environment similar to bulk [bmim][BF₄]. Hence, it may be concluded that the IL pools form when $R = 1.11$. Furthermore, the result has also revealed that the metal salt CoCl₂ can be solubilized into the nonaqueous IL/O microemulsion, which may be extended to some other metal species and perhaps even to other compounds. Thus, one can presume that the IL/O microemulsion has potential in the production of metallic and semiconductor nanomaterials.^[38]

MB has been considered to be an effective absorption probe for the investigation of nonionic reverse microemulsions.^[2] Figure 4 shows the effect of the successive addition

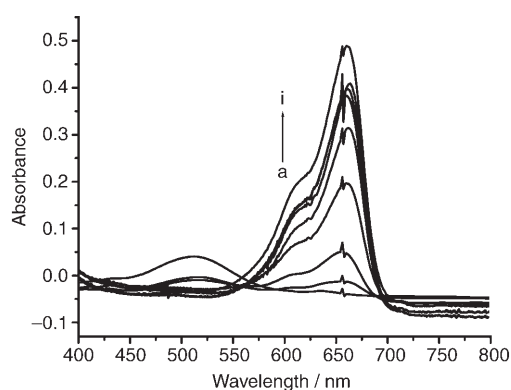


Figure 4. Absorbance spectra of MB in [bmim][BF₄]-in-benzene microemulsions given along line a in Figure 1 as a function of [bmim][BF₄] content with a) $R = 0$, b) 0.34, c) 0.71, d) 0.90, e) 1.11, f) 1.33, g) 1.55, h) 1.66, and i) pure IL. Probe concentration: 1.0×10^{-5} M.

of [bmim][BF₄] on the absorption spectra of MB in the TX-100/benzene binary system. The λ_{\max} value of MB in the TX-100/benzene mixture is 511 nm (Figure 4a), which is remarkably different from that of MB in pure [bmim][BF₄] ($\lambda_{\max} = 660$ nm; Figure 4i). It has already been suggested that the formation of a 1:1 complex between MB and TX-100 led to a remarkable blue shift of the MB absorption band.^[2,39] Therefore, the absorption band at 511 nm may be ascribed to the same complex in the TX-100/benzene mixture. On successively increasing the [bmim][BF₄] content, the band at the lower wavelength region ($\lambda_{\max} = 511$ nm) begins to disappear gradually and a concomitant increase in intensity at the higher wavelength region ($\lambda_{\max} = 660$ nm) is observed. The gradual decrease of the former band is due to the decrease in the amount of the 1:1 MB·TX-100 complex, whereas the increase of the latter band is ascribed to the fact that more and more MB molecules are dissolved into [bmim][BF₄], thus the amount of free MB is increased with increasing amounts of [bmim][BF₄]. Up to $R = 1.33$, the IL pools begin to form and MB is saturated with [bmim][BF₄]. Further increase in the amount of [bmim][BF₄] does not change the

microenvironment of MB, and thus the conformation of the band remains unchanged (Figure 4f–h). Our experimental phenomenon is similar to when water is used as the polar component.^[2] Thus, the formation of IL pools is further confirmed by the MB probe, that is, the IL pools begin to appear when $R = 1.33$, which is close to the value of 1.11, as revealed by the CoCl₂ probe.

Solubilization sites of MO: The absorption maximum λ_{\max} of MO is red shifted by increasing its local polarity.^[39,40] The polarity of water is remarkably different from that of [bmim][BF₄] and TX-100, therefore, it is feasible to use MO as a probe to indicate the solubilization sites of the added water. However, we had to first determine the solubilization sites of the absorption probe. It has been reported that MO molecules prefer to locate in the polar outer shells, composed of the hydrated OE chains of TX-100 in aqueous microemulsions, rather than solubilized in the water pools.^[39] Here, MO is insoluble in benzene but soluble in [bmim][BF₄] and pure liquid TX-100. Thus, in the [bmim][BF₄]-in-benzene microemulsions, MO can be considered to be completely solubilized in the polar cores of the IL/O microemulsion, which consist of polar outer shells (OE domain), polar IL pools, and benzene molecules that penetrate into the cores. The probe molecules can possibly partition between the two polar regions. To delineate the actual preferential locations of MO in the IL/O microemulsion, we simulated the environments found in the two regions by using TX-100/[bmim][BF₄] micellar solutions as the media for the probe. In such solutions, at TX-100 concentrations $C_{\text{TX-100}}$ above the critical micelle concentration (cmc; $\approx 7.73 \times 10^{-2}$ M), normal micelles form and these two polar environments are created. Figure 5 shows the absorption spectra of

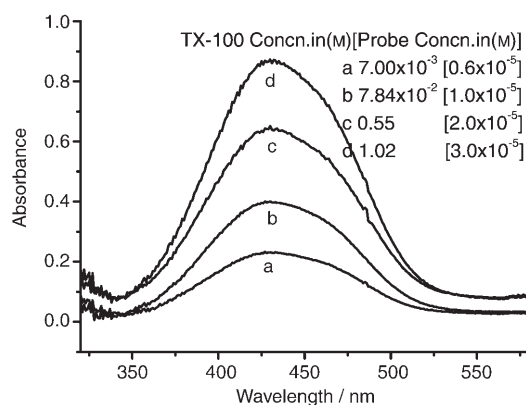


Figure 5. Absorption spectra of MO in the TX-100/[bmim][BF₄] solutions as a function of TX-100 concentration. The critical micelle concentration of TX-100 in [bmim][BF₄] was about 7.73×10^{-2} M and the λ_{\max} value was constant at 430 nm.

MO in solutions of [bmim][BF₄] at different $C_{\text{TX-100}}$ values. No micelles are present at $C_{\text{TX-100}} = 7.0 \times 10^{-3}$ M, and the λ_{\max} value of MO appears at 430 nm (Figure 5a), which is the same for bulk [bmim][BF₄], thus indicating that MO is

located in [bmim][BF₄]. However, after the normal micelles are formed (Figure 5b–d), no effect on the λ_{\max} value is observed, which indicates that MO is still in the bulk [bmim][BF₄] instead of being solubilized in the polar outer layer. Thus, one may presume that in the [bmim][BF₄]-in-benzene nonaqueous IL microemulsions, if IL pools are formed, the MO molecules will move from the polar outer shells (OE domain) into the IL pools.

The effect of the successive addition of [bmim][BF₄] on the microenvironment of the TX-100/benzene binary system is demonstrated by the UV/Vis spectra of MO (Figure 6).

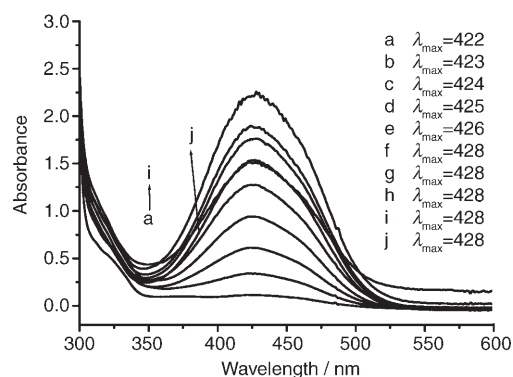


Figure 6. Absorbance spectra of MO in the [bmim][BF₄]-in-benzene nonaqueous IL microemulsions given along line a in Figure 1 as a function of [bmim][BF₄] content with a) $R=0.17$, b) 0.34, c) 0.52, d) 0.71, e) 0.90, f) 1.11, g) 1.33, h) 1.55, i) 1.66, and j) 1.79. Probe concentrations: a) 1.0×10^{-5} , b) 1.5×10^{-5} , c) 2.0×10^{-5} , d) 2.5×10^{-5} , e) 3.0×10^{-5} , f) 3.5×10^{-5} , g) 4.0×10^{-5} , h) 4.5×10^{-5} , i) 5.5×10^{-5} , and j) 3.5×10^{-5} M, respectively.

The red shift in the λ_{\max} value from 422 to 426 nm when $R=0.17$ –0.90 indicates that the polarity of the microdomain increases, whereas with further increasing [bmim][BF₄] at $R > 1.11$ no more change in micropolarity is reported by MO, and the λ_{\max} value always remains constant (428 nm) until the isotropic microemulsion system attains the phase-separation point. A possible reason for this behavior may be that at small but increasing R values [bmim][BF₄] molecules are dispersed in the polar cores (only OE domain herein) to bind the OE groups of TX-100 in which the MO molecules are still embedded. The gradually increasing micropolarity is reflected by a red shift of the λ_{\max} value (422–426 nm) as a result of the successive addition of [bmim][BF₄]. After the binding of [bmim][BF₄] an equilibrium is reached and subsequently added IL molecules begin to accumulate in the core of the reverse microemulsion to form IL pools, and thus the MO molecules move from the polar outer shells (OE domain) into the IL pools. The polarity of the IL pools is greater than that of the polar outer shells, therefore the λ_{\max} value of MO presents a larger value, namely 428 nm.

In traditional aqueous microemulsions, bound water molecules have a restricted mobility and lack of the normal hydrogen-bonded structure and thus contribute to a low polarity.^[29,41] The polarity of the microemulsion polar cores is eventually dominated by the competitive contribution from

two types of water molecules, bound water, and free water.^[42] Generally, the polarity of the water pools is much lower than that of bulk water and changes evidently with increasing water content. However, the polarity of the IL pools remains constant and close to the bulk IL for the current IL/O microemulsion. A possible reason for this behavior is that the IL molecules are bonded to the OE groups of TX-100 through weak electrostatic interactions between the electropositive imidazolium rings and the electronegative oxygen atoms of the OE groups in TX-100.^[28] The electrostatic interactions are so much weaker relative to hydrogen-bonding interactions that the properties of [bmim][BF₄] would not be affected as greatly as those of the bound water in aqueous microemulsions.

Solubilization of water: Over the years, efforts have been made to understand the details of water molecules solubilized in heterogeneous media, both experimentally and theoretically.^[43,44] Understanding the properties of water in confined media has a direct relevance to biological systems.^[45] In addition, it is also important to study the states or properties of solubilized water in microemulsion media under different conditions to understand how the changes in the microenvironment affect the morphology and properties of materials.^[46–49] It has been reported that when water is added to the TX-100-based reverse micellar solutions at low concentrations most of the water molecules are bound to the OE groups, but more and more water molecules are present in the free form in water pools at higher water concentrations.^[50] However, water is also highly soluble in [bmim][BF₄]. In this case, if water is added to the IL/O reverse microemulsion, the solubilization sites of the water molecules are still unclear.

UV/Vis spectra: To describe their actual preferential locations, UV/Vis spectroscopic analysis with MO as an absorption probe was also used for insight into the change in the microenvironment of the IL/O microemulsion. In the IL/O microemulsion with $R=1.33$, the IL pools appear in the polar cores and the MO molecules are located in the IL pools. The original addition of water to the system does not lead to any change in the λ_{\max} value (428 nm, not shown herein), thus reflecting that the polarity of the IL pools remains unchanged. This result suggests that these water molecules are located in the polar outer shells to bind the OE groups of TX-100. With a water content of up to 3.8 wt% of the IL microemulsion, the λ_{\max} value red shifts gradually, thus indicating that the polarity of the IL pool is increased. This behavior results when the bound water in the polar outer shells reaches saturation, and subsequently added water molecules begin to enter the IL pools. The polarity of water is greater than that of [bmim][BF₄], therefore the polarity of the IL pools is enhanced.

Unexpectedly, it was discovered that small amounts of added water does not accelerate the phase separation, even for the investigated microemulsion system near the phase-separation points. Instead, the added water possibly makes

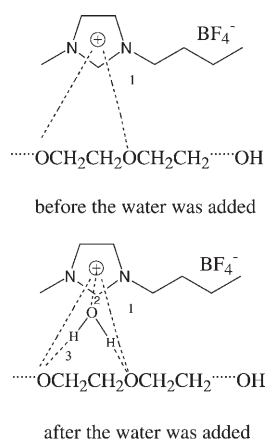


Figure 7. Two-dimensional simplified model of the interaction between [bmim][BF₄], H₂O, and the hydrophilic tail (OE units) of TX-100. 1) Weak electrostatic interaction between the electronegative oxygen atoms of the units and the electropositive imidazolium rings. 2) Electrostatic interaction between the electronegative oxygen atoms of water and the electropositive imidazolium rings. 3) Hydrogen-bonding interactions between the hydrogen atoms of the water molecules and the electronegative oxygen atoms of the OE units in TX-100.

the IL/O microemulsion more stable. In our previous study, we found that the driving force for solubilizing IL into the cores of the TX-100 aggregates may be the weak electrostatic interaction between the electronegative oxygen atoms of the OE units in TX-100 and the electropositive imidazolium rings.^[28] When water is added to the IL/O microemulsion, the water molecules are inclined to form hydrogen-bonding interactions with the electronegative oxygen atoms of the OE units in TX-100, and at the same time the electronegative oxygen atoms of water electrostatically attract the electropositive imidazolium rings. Both the hydrogen-bonding and electrostatic interactions are much stronger than the electrostatic interaction between the oxygen atoms of the OE units and the electropositive imidazolium rings because the electronegativity of the oxygen atoms in water is stronger than that of the oxygen atoms in the OE units.^[51] The interaction relations before and after water is added are shown in Figure 7.

Evidently, these added water molecules can be considered to be a glue that sticks the IL and OE units of TX-100 more tightly together. Therefore, the microemulsion stability is actually enhanced, which has been confirmed by the fact that more IL can be solubilized into the microemulsion in the presence of water.

FTIR spectra: FTIR spectroscopy is an important tool for determining the extent of the hydrogen bonding present and thus reflects some structural information on the microemulsions.^[52] Free and hydrogen-bonded species have molecular vibrations at different IR frequencies.^[51] Therefore, FTIR spectroscopic analysis is the most widely used method to investigate the states of solubilized water and the structures of traditional aqueous microemulsions.^[29,34,53–55] The characteristics of the water molecules incorporated into reverse micelles depend strongly on the water content and the nature of the surfactant headgroups.^[56] Generally, solubilized water molecules in microemulsions have three distinct states: trapped water, bound water, and free water. The trapped water, with the O–H stretching vibration at about 3600 cm⁻¹, is defined as the water species dispersed among the long hydrocarbon chains of the surfactant molecules.^[29] This trapped water exists as monomers (or dimers) and has no hydrogen-

bonding interactions with the surroundings. Furthermore, a small amount of water dissolved in a nonpolar solvent is also considered to be trapped water.^[34] In the TX-100-based micelles, a larger number of water molecules are located in the palisade layer, and these water molecules are either just mechanically trapped within the micellar structure or thermodynamically bound to the OE groups through intermolecular hydrogen-bonding interactions. Amongst the mechanically trapped water molecules, some are intermolecularly hydrogen bonded with themselves and some are free.^[45] As the trapped water molecules are matrix-isolated dimers or monomeric in nature, they absorb in the high-frequency region.^[29] The bound water molecules form hydrogen-bonding interactions with the polar headgroups of the surfactants, thus resulting in absorption in the low-frequency region of the IR spectrum. For the nonionic TX-100 formed W/O microemulsions, the O–H stretching vibration of the bound water appears at 3400 ± 20 cm⁻¹.^[54] Considering that the polar outer shells of the investigated IL/O microemulsion are similar to the palisade layers of TX-100 micelles, it is possible that the water molecules in the IL/O microemulsion are either mechanically trapped in the microemulsion or thermodynamically bound to the OE units. Apart from these two types of water species, the free water molecules, which occupy the core of the surfactant aggregates, have strong hydrogen-bonding interactions amongst themselves, that is, they have similar bulk-water properties, thus shifting the O–H stretching band to a lower frequency of 3220 ± 20 cm⁻¹.^[54]

FTIR spectroscopic analysis of the [bmim][BF₄]-in-benzene microemulsion along line a with *R* = 1.33 as a function of the added water content was carried out. Only the bands of O–H stretching (3200–3600 cm⁻¹) and C–H imidazolium-ring stretching (3090–3160 cm⁻¹) change significantly with the added water. The O–H stretching band originally appears at 3426 cm⁻¹, which is due to the terminal O–H group of TX-100, and remarkably shifts to 3477 cm⁻¹ when the water content reaches up to 1.1 wt % of the microemulsion system. After that, the wavenumber of the O–H stretching band almost remains unchanged when the water content is in the range 1.1–2.2 wt %. Finally, a gradual decrease in wavenumber is observed on increasing the water content further (see Figure 8). A possible reason for this behavior is that when water is just added to the microemulsion, as mentioned above, these water molecules are either mechanically trapped in the microemulsion or thermodynamically bound to the OE units of TX-100 by hydrogen-bonding interactions. Moreover, it has been reported that the number of trapped water exhibits no significant change; however, the bound water molecules increase gradually with the rising water content.^[53] This behavior means that the equilibrium of the trapped water dispersed within the microemulsion system is achieved almost instantaneously. Thus, we can presume that the water molecules prefer to be trapped in the microemulsion first. Owing to the O–H high-frequency stretching vibration of the trapped water, the total O–H stretching band moves to a high-frequency region rapidly.

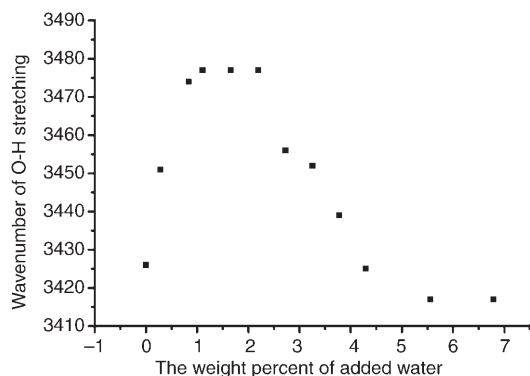


Figure 8. Dependence of the O–H stretching frequencies of the IL/O microemulsion along line a with $R=1.33$ on the added water content (wt%).

Meanwhile, the number of bound water molecules with the O–H stretching vibration at $3400 \pm 20 \text{ cm}^{-1}$ always increases. This O–H stretching vibration is close to that of the terminal O–H stretching vibration of TX-100 (3426 cm^{-1}), thus leading to the appearance of a wavenumber platform which then declines. If free water appears in our investigated microemulsion, considering the low-frequency vibration of free water ($3220 \pm 20 \text{ cm}^{-1}$), the total O–H stretching band will move to a fairly low-frequency region. No free water is present in our investigated water-content range. Actually, the required free-water content of the nonionic TX-100-supported microemulsions is much higher than that of the ionic surfactant microemulsions owing to the fairly long hydrophilic chains of TX-100. In addition, when the water content is above 3.8 wt% of the microemulsion, the wavenumber of the C–H imidazolium-ring stretching suddenly moves to a low-frequency region, which is caused by the electrostatic attraction of the electronegative oxygen atoms of the water molecules. This result indicates that water molecules begin to enter the IL pools, which is in accordance with that shown by the UV/Vis spectroscopic analysis.

FTIR spectroscopic analysis has shown that when a small amount of water is added to the IL/O microemulsion, the water molecules are inclined to be first trapped and bound into the polar outer shells of the microemulsion. It can be realized that this unique solubilization behavior provides an aqueous interface, and thus the IL/O microemulsion may be used as a medium for the preparation of porous or hollow nanomaterials by hydrolysis reactions.

¹H NMR spectroscopy: ¹H NMR spectroscopic analysis gives more detailed information about the interaction between the molecules and thus provides insight into the solubilization information of added water molecules in the polar cores of the IL/O microemulsions. In our previous report, ¹H NMR spectroscopic analysis was used to investigate the microstructure characteristics of the IL microemulsions.^[28] The experimental results showed that on increasing the IL content to the micelles, all the proton signals of the OE units of TX-100 were affected by the added [bmim][BF₄],

and these signals appeared in a downfield position. Furthermore, the signals of H-1, H-2, and H-3 in the imidazolium rings of [bmim][BF₄] were also gradually shifted downfield under the ring-current effect. The results revealed that the electron density of the oxygen atoms of the OE units electrostatically attracted the electropositive imidazolium rings and that the electrostatic interaction was considered to be the driving force for solubilizing IL into the core of the TX-100 aggregates.^[28]

In this section, deuterated water replaces H₂O and the effect of the water content on the microenvironment of the IL/O microemulsion is investigated by ¹H NMR spectroscopic analysis. Figure 9 shows the ¹H NMR spectra of the [bmim][BF₄]-in-benzene microemulsion with $R=1.33$ and various water contents. The addition of water affects the

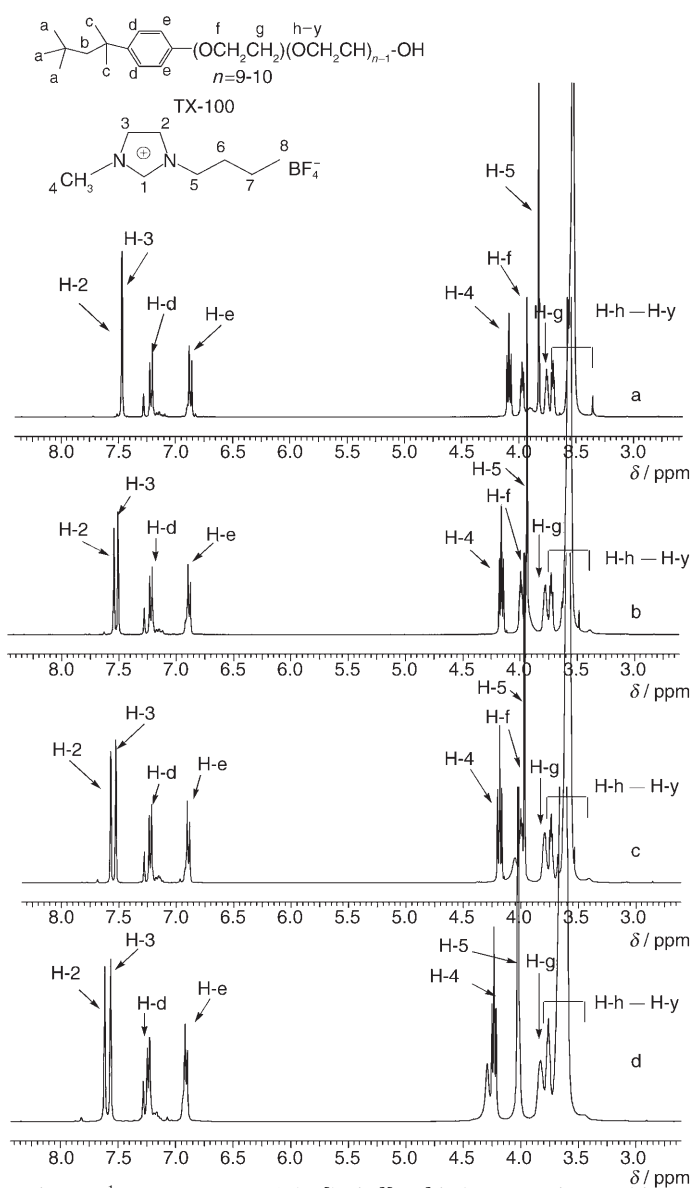


Figure 9. ¹H NMR spectra of the [bmim][BF₄]-in-benzene microemulsion along line a with $R=1.33$ at various water contents: a) 0, b) 1.6, c) 3.8, and d) 5.6 wt% of the microemulsion system.

conformation of many signals. The signals of H-2 and H-3 in [bmim][BF₄], which overlap owing to a similar chemical environment and are centered at $\delta=7.47$ ppm, gradually split into two duplet peaks and the distance between these two peaks becomes larger and larger with a successively increasing water content; meanwhile, the triplet peak of the H-f signal of the OE units at $\delta=3.98, 3.97,$ and 3.96 ppm overlap into an unresolved peak centered at $\delta=4.03$ ppm with a water content of up to 5.6 wt % of the microemulsion. Similarly, the ternary peaks of the H-g signal of the OE units, which resonate at $\delta=3.76$ and 3.75 ppm, have combined to give one peak at $\delta=3.83$ ppm. More remarkably, the other proton signals of the OE units in TX-100, which overlap into a strong and unresolved single peak as a result of a similar environment, become broader and broader with a successively increasing water content. These changes suggest that there are some interactions between the added water molecules and [bmim][BF₄] as well as the TX-100 molecules. The interaction has affected the chemical shifts of many signals. When the added water content is in the range 1.6–5.6 wt % of the microemulsion, the two ternary peaks of the H-2 signals of [bmim][BF₄] shift downfield from $\delta=7.522, 7.517,$ and $7.493, 7.489$ ppm to $\delta=7.616, 7.612$ and $7.565, 7.560$ ppm, respectively. The shifts experienced by the H-2 and H-3 resonances are downfield because the electronegative oxygen atoms of the added water molecules tend to attract the electropositive imidazolium rings, and thus the electropositivity of the imidazolium ring is decreased. However, under the ring-current effect, the small magnetic field is the reverse of the external magnetic field, but on the side of aromatic rings the orientation of the small magnetic field is in accord with the external magnetic field. Therefore, the external magnetic field is actually enhanced and H-2 and H-3, which are on the side of the aromatic imidazolium rings, are deshielded. After water is added, the electron density on the imidazolium rings increases and the deshielding is enhanced, therefore the H-2 and H-3 signals shift further downfield.^[28] Although H-1 is also on the imidazolium ring in [bmim][BF₄], the proton signal shows a very strong Lewis acidity and other influential factors make the signal shift irregularly.

In addition, all the proton signals of the OE units in TX-100 shift downfield owing to the addition of water. The triple peaks of H-f that originally resonated at $\delta=3.98, 3.97,$ and 3.96 ppm move to a downfield position centered at $\delta=4.03$ ppm when the water content is up to 5.6 wt % of the microemulsion. At the same time, the triplet of peaks that appear at $\delta=3.71, 3.70,$ and 3.69 ppm, ascribed to H-g of the OE units, move to a downfield position centered at $\delta=3.76$ ppm. The other proton signals of the OE units, reflected by a broad peak, shift from $\delta=3.52$ to 3.64 ppm. The downfield shift experienced by the OE proton resonances may be a result of the added water molecules forming hydrogen-bonding interactions to the OE units, and thus the electron density on the oxygen atoms of the OE units is decreased. The electropositivity of the carbon atoms adjacent to the oxygen atoms is enhanced owing to the induction

effect. As a consequence, the hydrogen atoms on the carbon atoms are deshielded and resonate in a downfield position.

Furthermore, it is worthy of note that a new broad peak at $\delta=3.80$ ppm is observed on successively adding water up to 1.6 wt % of the microemulsion system. The peak becomes stronger and stronger and shifts downfield gradually to $\delta=4.29$ ppm when the water content is up to 5.6 wt %. The new peak is actually ascribed to the added water molecules because the proton exchange will happen between D₂O and the terminal hydroxy groups of TX-100, thus leading to the appearance of H₂O molecules. Besides, there are also some water molecules doped in the D₂O reagent. The reason for the downfield shift may be that with increasing water content the amount of OE units surrounding the water molecules is relatively decreased, thus deshielding is weakened. Furthermore, the broad single peak for the solubilized water

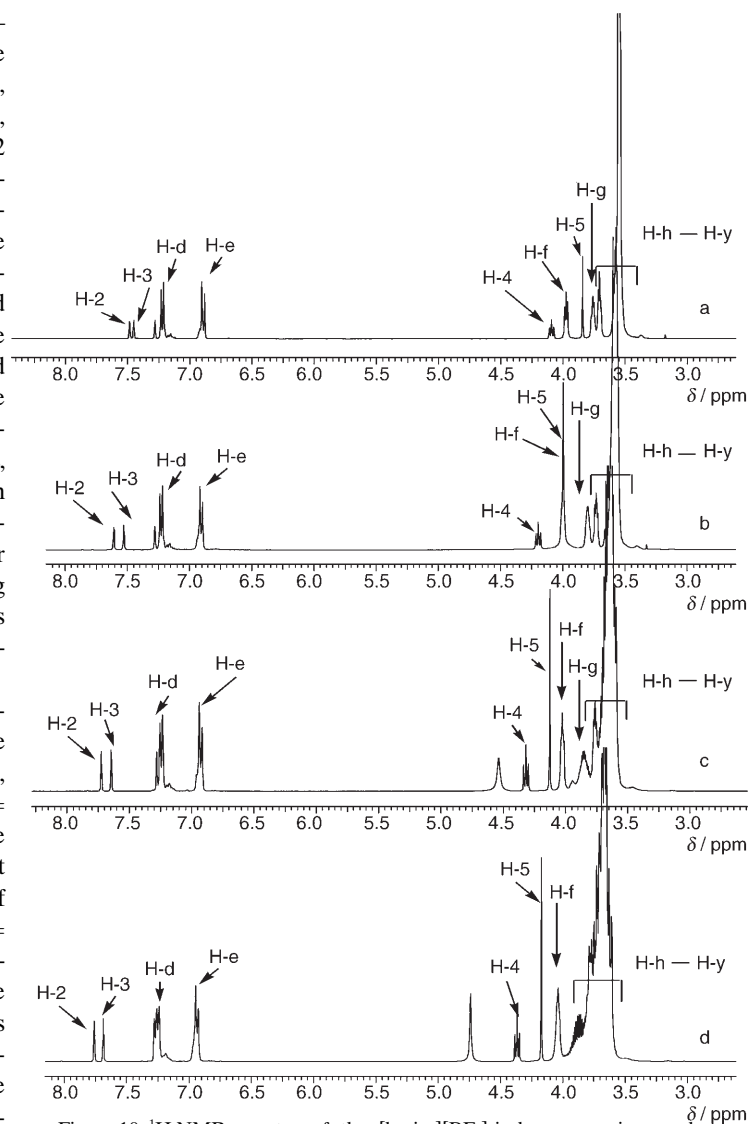


Figure 10. ¹H NMR spectra of the [bmim][BF₄]-in-benzene microemulsion along line a with $R=0.34$, the other conditions are the same as those in Figure 9.

indicates the rapid exchange between the water protons at various states.^[34]

The effect of water content on another IL/O microemulsion with $R=0.34$ was also investigated by ^1H NMR spectroscopic analysis under the same conditions. Briefly, no IL pools are present in the investigated system. The ^1H NMR spectra of the microemulsion with various water contents are shown in Figure 10. Similar results are obtained relative to the former microemulsion system, but the effect of added water on the latter is greater than the former, as reflected by greater changes in the signal conformation and chemical shift in the latter case. A possible reason for this behavior is that the surfactant chains are not fully extended or ordered in the latter microemulsion.^[36] Every water molecule is thus fully encircled by the surrounding OE units of TX-100. However, in the latter case, the microemulsion is further swollen and the increase of IL induces a greater degree of order into the OE chains, as deduced from the decrease in hydrogen bonding between the terminal hydroxy groups of TX-100 and the oxygen atoms of the OE units.^[28] Thus, the number of surrounding OE units is relatively decreased, that is, the same amount of water molecules in the latter system has a greater effect on the surrounding OE units; therefore, the changes in the ^1H NMR spectra in the latter induced by added water are more remarkable. A schematic representation of the water molecules in two different microenvironments is shown in Figure 11.

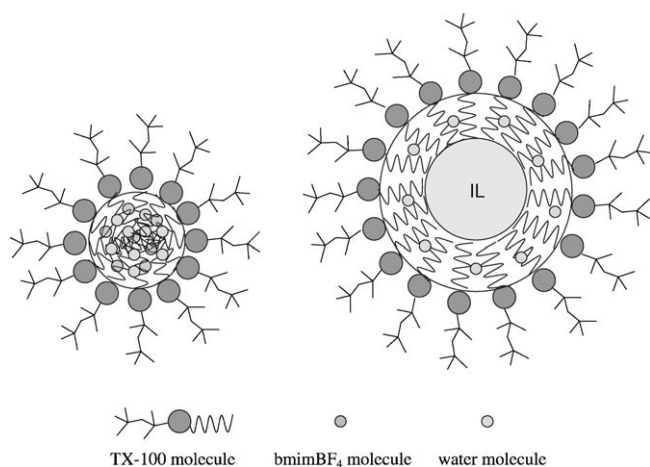


Figure 11. A schematic representation of water molecules in two different microenvironments. a) IL/O microemulsion without IL pools; b) IL/O microemulsion with an IL pool.

Conclusion

Microemulsions consisting of $[\text{bmim}][\text{BF}_4]$, surfactant TX-100, and benzene were prepared, and the phase behavior of the ternary system was investigated. DLS revealed that with increasing amounts of added $[\text{bmim}][\text{BF}_4]$ the size of the aggregates increased, which were similar to those of typical W/O microemulsions, thus suggesting the formation of an IL/O

microemulsion. The micelles became swollen on successively adding $[\text{bmim}][\text{BF}_4]$ to the system, and IL pools formed when the $[\text{bmim}][\text{BF}_4]$ content was more than 1.11 wt% of the IL microemulsion system, as confirmed by UV/Vis spectroscopic analysis with CoCl_2 and MB as the absorption probes. The effect of added water on the microstructures of the IL/O microemulsions was discussed. First, it was found that the UV/Vis absorption probe MO tended to locate in the interior of the IL pool. A constant polarity was obtained in the IL pool, even if a small amount of water was added to the microemulsion, thus indicating that the water molecules were solubilized in the polar outer shells. These water molecules, through hydrogen-bonding interactions with the oxygen atoms of the OE units of TX-100 and electrostatic attraction to the electropositive imidazolium rings, act as a glue that sticks the IL and OE units more tightly, thus making the microemulsion more stable. FTIR spectra revealed that the added water molecules were inclined to be first solubilized in the polar outer shells as bound and trapped water. The interaction between the added water and their surroundings was further confirmed by ^1H NMR spectroscopic analysis. The unique solubilization behavior of water provided an aqueous interface, and thus the IL/O microemulsion may be applied to the preparation of porous or hollow nanomaterials by hydrolysis reactions.

Acknowledgements

We are grateful to the National Natural Science Foundation of China (No. 50472069) and the Department of Science and Technology of Shandong Province (Z2004B02). We thank Prof. Yebang Tan (Shandong University) for his help with the ^1H NMR spectroscopic analysis and Prof. S. E. Friberg (University of Virginia) for his encouragement throughout the course of this investigation.

- [1] M. Schwuger, K. Stickdorn, R. Schomaecker, *Chem. Rev.* **1995**, *95*, 849–864.
- [2] L. M. Qi, J. M. Ma, *J. Colloid Interface Sci.* **1998**, *197*, 36–42.
- [3] K. Holmberg, *Adv. Colloid Interface Sci.* **1994**, *51*, 137–174.
- [4] S. E. Friberg, M. Podzimek, *Colloid Polym. Sci.* **1984**, *262*, 252–253.
- [5] I. Rico, A. Lattes, *Nouv. J. Chim.* **1984**, *8*, 429–431.
- [6] P. D. I. Fletcher, M. F. Gokal, B. H. Robinson, *J. Chem. Soc. Faraday Trans. 1* **1984**, *80*, 3307–3314.
- [7] S. E. Friberg, Y. C. Liang, *Surfactant Sci. Ser.* **1987**, *24*, 103–105.
- [8] I. Rico, A. Lattes, *Surfactant Sci. Ser.* **1987**, *24*, 357–360.
- [9] A. Martino, E. W. Kaler, *J. Phys. Chem.* **1990**, *94*, 1627–1631.
- [10] R. D. Falcone, N. M. Correa, M. A. Biasutti, J. J. Silber, *Langmuir* **2000**, *16*, 3070–3076.
- [11] K. P. Das, A. Ceglie, B. Lindman, *J. Phys. Chem.* **1987**, *91*, 2938–2946.
- [12] I. Rico, A. Lattes, *J. Colloid Interface Sci.* **1984**, *102*, 285–287.
- [13] A. Lattes, I. Rico, A. de Savignac, A. Ahmad-Zadeh Samii, *Tetrahedron* **1987**, *43*, 1725–1735.
- [14] K. Holmberg, B. Lassen, M. B. Stark, *J. Am. Oil Chem. Soc.* **1989**, *66*, 1796–1800.
- [15] A. Lattes, I. Rico, *Surfactant Sci. Ser.* **1987**, *24*, 377–382.
- [16] A. Lattes, I. Rico, *Colloids Surf.* **1989**, *35*, 221–235.
- [17] K. P. Das, A. Ceglie, B. Lindman, *J. Phys. Chem.* **1987**, *91*, 2938–2946.
- [18] P. D. I. Fletcher, R. B. Freedman, B. H. Robinson, G. D. Rees, R. Schomäcker, *Biochim. Biophys. Acta* **1987**, *912*, 278–282.

- [19] K. V. Schubert, K. M. Lusvardi, E. W. Kaler, *Colloid Polym. Sci.* **1996**, *274*, 875–883.
- [20] I. Rico, A. Lattes, *J. Am. Chem. Soc.* **1989**, *111*, 7266–7267.
- [21] J. Planeta, M. Roth, *J. Phys. Chem. B* **2004**, *108*, 11244–11249.
- [22] T. Welton, *Chem. Rev.* **1999**, *99*, 2071–2083.
- [23] J. Dupont, R. F. de Souza, P. A. Z. Suarez, *Chem. Rev.* **2002**, *102*, 3667–3692.
- [24] J. F. Liu, G. B. Jiang, Y. G. Chi, Y. Q. Cai, Q. X. Zhou, J. T. Hu, *Anal. Chem.* **2003**, *75*, 5870–5876.
- [25] H. X. Gao, J. C. Li, B. X. Han, W. N. Chen, J. L. Zhang, R. Zhang, D. D. Yan, *Phys. Chem. Chem. Phys.* **2004**, *6*, 2914–2916.
- [26] J. Eastoe, S. Gold, S. E. Rogers, A. Paul, T. Welton, R. K. Heenan, I. Grillo, *J. Am. Chem. Soc.* **2005**, *127*, 7302–7303.
- [27] D. Chakrabarty, D. Seth, A. Chakraborty, N. Sarkar, *J. Phys. Chem. A* **2005**, *109*, 5753–5758.
- [28] Y. A. Gao, J. Zhang, H. Y. Xu, X. Y. Zhao, L. Q. Zheng, X. W. Li, L. Yu, *ChemPhysChem* **2006**, *7*, 1554–1561.
- [29] T. K. Jain, M. Varshney, A. Maitra, *J. Phys. Chem.* **1989**, *93*, 7409–7416.
- [30] J. Dupont, C. S. Consorti, P. A. Z. Suarez, R. F. Souza, *Org. Synth.* **1999**, *79*, 236–241.
- [31] C. Mo, *Langmuir* **2002**, *18*, 4047–4053.
- [32] S. Nave, J. Eastoe, R. K. Heenan, D. Steytler, I. Grillo, *Langmuir* **2000**, *16*, 8741–8748.
- [33] D. M. Zhu, X. Wu, Z. A. Schelly, *J. Phys. Chem.* **1992**, *96*, 7121–7126.
- [34] N. F. Zhou, Q. Li, J. Wu, J. Chen, S. Weng, G. Xu, *Langmuir* **2001**, *17*, 4505–4509.
- [35] G. B. Dutt, *J. Phys. Chem. B* **2004**, *108*, 7944–7949.
- [36] H. Christenson, S. E. Friberg, D. W. Larsen, *J. Phys. Chem.* **1980**, *84*, 3633–3638.
- [37] A suitable amount of cyclohexane was added to the mixture of TX-100 and benzene to make the micelles appear because TX-100-based micelles could not be formed when benzene was used as the only solvent in the absence of a polar component.
- [38] Y. A. Gao, N. Li, L. Q. Zheng, X. Y. Zhao, S. H. Zhang, B. X. Han, W. G. Hou, G. Z. Li, *Green Chem.* **2006**, *8*, 43–49.
- [39] D. Pramanick, D. Mukherjee, *J. Colloid Interface Sci.* **1993**, *157*, 131–134.
- [40] D. M. Zhu, Z. A. Schelly, *Langmuir* **1992**, *8*, 48–50.
- [41] M. Wong, J. K. Thomas, M. Gratzel, *J. Am. Chem. Soc.* **1976**, *98*, 2391–2397.
- [42] R. E. Riter, E. P. Undiks, J. R. Kimmel, N. E. Levinger, *J. Phys. Chem. A* **1998**, *102*, 7931–7938.
- [43] K. Bhattacharyya, B. Bagchi, *J. Phys. Chem. A* **2000**, *104*, 10603–10613.
- [44] N. Nandi, K. Bhattacharyya, B. Bagchi, *Chem. Rev.* **2000**, *100*, 2013–2046.
- [45] M. Kumbhakar, T. Goel, T. Mukherjee, H. Pal, *J. Phys. Chem. A* **2004**, *108*, 19246–19254.
- [46] S. Lee, D. F. Shantz, *Chem. Mater.* **2005**, *17*, 409–417.
- [47] J. L. Lemyre, A. M. Ritcey, *Chem. Mater.* **2005**, *17*, 3040–3043.
- [48] M. Roth, R. Hempelmann, *Chem. Mater.* **1998**, *10*, 78–82.
- [49] D. H. Chen, S. H. Wu, *Chem. Mater.* **2000**, *12*, 1354–1360.
- [50] C. Kumar, D. Balasubramanian, *J. Colloid Interface Sci.* **1980**, *74*, 64–70.
- [51] A. J. Thote, R. B. Gupta, *Ind. Eng. Chem. Res.* **2003**, *42*, 1129–1136.
- [52] P. L. Brinkley, R. B. Gupta, *AIChE J.* **2001**, *47*, 948–953.
- [53] G. W. Zhou, G. Z. Li, W. J. Chen, *Langmuir* **2002**, *18*, 4566–4571.
- [54] H. X. Zeng; Z. P. Li, H. Q. Wang, *Acta Physico-Chimica Sinica*, **1999**, *15*, 522–526.
- [55] Q. Li, S. F. Weng, J. G. Wu, N. F. Zhou, *J. Phys. Chem. B* **1998**, *102*, 3168–3174.
- [56] Q. Li, T. Li, J. G. Wu, *J. Phys. Chem. B* **2000**, *104*, 9011–9016.

Received: July 3, 2006
Published online: December 19, 2006